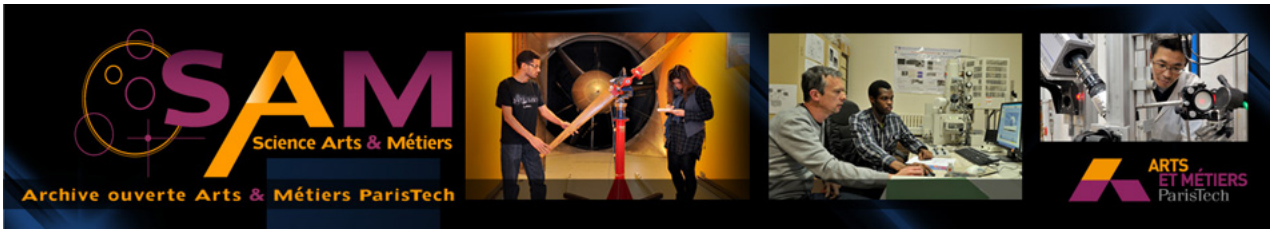

Effect of O_2 increase on properties of vanadium oxide coatings

A. Zairi*[1,2], A. Ben Cheikh Larbi[1], A. Iost[2] and M. H. Staia[2]

The present research was carried out with the aim of studying the influence of oxygen concentration during processing on the properties of the VO_x coatings deposited by cathodic magnetron sputtering on a stainless steel AISI 316L substrate. Mechanical and tribological properties were measured by nanoindentation and sliding wear tests respectively. Adhesion was evaluated by means of the scratch test. In order to determine the texture of the coatings, complementary characterization methods including X-ray diffraction in grazing incidence and Bragg Brentano configurations, as well as Ω scans, were performed. It was found that the texture of the crystalline coatings is strongly influenced by the amount of partial pressure of oxygen in the reactor atmosphere. The V_2O_5 phase, with an orthorhombic symmetry, was produced in the coating, which had a pronounced texturing for the (001) plane, exhibiting the best values of hardness and Young modulus. It was shown that, as the oxygen concentration drops to <1 sccm, the mechanical and tribological characteristics, as well as the coating adhesion, tend to decrease considerably.

Keywords: Vanadium oxides, Structural properties, Mechanical properties, Tribological properties, Adhesion

Introduction

Coatings of vanadium oxides are particularly suitable for many applications, and their use in optical, electronic and photonic industries has implied an extensive research related to the improvement of their optical and magnetic properties.[1,2] However, only few researches have been performed until now to study their mechanical and tribological performance, although they exhibit some very attractive features, such as self-lubrication attributes, especially at high temperatures.

The diversity of applications is dictated by the multiplicity of phases that the V–O system can generate with multiple stoichiometries, such as Magneli and crystalline phases that can be obtained as, for example, V_2O_3, VO_2 and V_2O_5.[3] Particularly, the V_2O_5 phase is desired for its structural stability.

The performance of VO_x thin films has been greatly improved using different deposition technologies such as cathodic reactive sputtering,[4–6] pulsed laser deposition,[7] evaporation[8,9] and chemical vapour deposition.[10] Each method provides the thin film with specific properties consistent with its growth mechanism, the corresponding texture and the associated mechanical properties.[11] In addition, it is recognized that control of oxygen partial pressure, temperature and the nature of the substrate has a direct effect on the structure and functionality of the coatings. Several studies have been conducted to determine the influence of oxygen on the coating structure when varying the flowrate during processing.[12,13]

The present work fits into this framework and aims to elucidate both effects of oxygen flow on the coating structure as well as the mechanical and tribological properties of vanadium oxide obtained by physical vapour deposition (PVD). Since the adhesion of thin films to a substrate is a key factor for their use,[14] this study includes an analysis of the effects of oxygen flow on the coating adhesion. The optimal composition of VO_x thin films is also discussed.

Experimental

The deposition of VO_x coatings was performed by PVD magnetron sputtering in continuous current mode and in a reactive atmosphere (ICMP, EPF Lausanne) on a stainless steel AISI 316L substrate. The target was vanadium of 99·5% purity. Direct current was maintained at 100 W. The substrate temperature during deposition was 400°C, which was deemed sufficient to generate a Magnéli phase (V_2O_5).[3] In order to obtain coatings that adhered to the substrate, a preliminary study showed the need of depositing a Ti adhesion interlayer with a thickness of 40 nm.[15] The Ti target had a purity of 99·99%. The processing conditions are described in Table 1.

The films were analyzed by X-ray diffraction on a Seifert ID 3003 (ICMP, EPF Lausanne) with a grazing incidence geometry $\Omega=4^\circ$. The same equipment was

[1]Ecole Nationale Supérieure des Ingénieurs de Tunis, LMMP – 5, Avenue Taha Hussein, 1200 Bab Mnara Montfleury, Tunisie
[2]Arts et Metiers ParisTech - MSMP, 8 Boulevard Louis XIV, F-59046 Lille, France

*Corresponding author, email amal.zairi@gmail.com

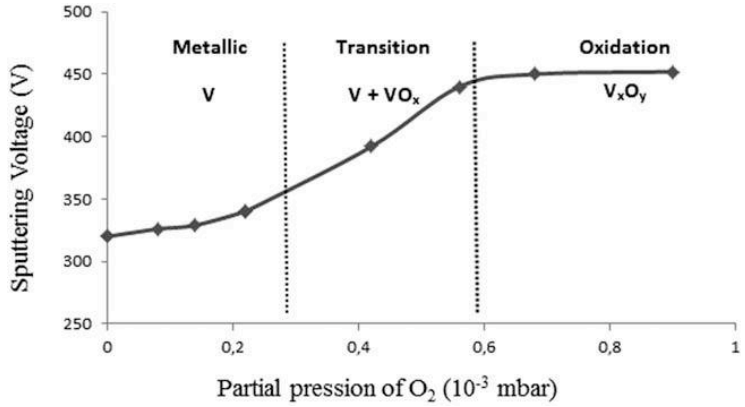

1 Voltage evolution as function of oxygen partial pressure

then used with a Bragg Brentano geometry to evaluate the texture.

The mechanical properties, i.e. the hardness and the Young modulus of the as deposited films, were determined from nanoindentation tests performed on a Nanoindenter XP (ICMP, EPF Lausanne) equipped with a Berkovich tip. The Oliver–Pharr method was used to deduce the hardness and Young modulus of the specimens from the unloading curve.[16]

The wear resistance and the friction behaviour of the PVD coatings were evaluated by sliding wear testing by means of an alternative tribometer TRIBOtechnic (MSMP, ENSAM-Lille). The normal load was 5 N, the sliding speed was 0·05 m s^{-1} and the sliding distance was 20 m. The ball on a plane configuration was used. The friction coefficient was monitored online during the tests. The worn volume was evaluated by means of an optical profilometer Wyko (MSMP, ENSAM-Lille).

The adhesion of the coatings was determined by scratch testing on a 'Scratch Test Millennium 200' (MSMP, ENSAM-Lille) machine equipped with an optical microscope, a system for detecting the acoustic emission and a tangential force sensing system. The combination of acoustic effects obtained with the variations in tangential forces during the scratching and the micrographs revealed various types of damage and the associated critical forces. It is known that these critical forces are numerous and have various origins. They generally correspond sequentially to a cohesive failure (Lc_1) and then an adhesive one (Lc_2) and are finally followed by the total damage of the coating (Lc_3).[17–20]

Results and discussion

Based on the fact that the pressure of the reactive gas flow significantly influences the generation of different phases of vanadium oxides, experimental investigations were conducted to vary the pressure while maintaining the other process parameters constant, as shown in Table 2. In fact, control of the target voltage is a feasible way of regulating the target oxidation. The flow of O_2 was gradually modified and correlated with the generation of different V_xO_y phases. Figure 1 presents the variation of the target voltage as a function of the partial pressure of O_2 obtained under these conditions.

As can be observed from Fig. 1, the nature of the phases will depend on the target surface state, a fact that was also shown recently by Wei *et al.*[21] Three different behaviours of voltage target during presputtering can be distinguished. First, no significant evolution of target voltage until a partial pressure of $\sim 0{\cdot}2 \times 10^{-3}$ mbar was achieved. The target is still in its metallic state.

However, by increasing the oxygen partial pressure, the voltage in the target begins to rise, and this moment corresponds to a transition mode, when the target begins to be oxidized. Hence, it was determined that the partial pressure of saturation corresponds to $0{\cdot}6 \times 10^{-3}$ mbar, a value representing the threshold at which this study was conducted.

This corresponds to a magnitude of 0·6 sccm of oxygen in the deposition chamber, and as it will be shown below, it allowed the production of a polycrystalline phase of V_2O_5, which is the main objective of the present research.

Therefore, in this study, it was decided to employ oxygen flowrates, which varied between 0·6 and 1·6 sccm, since under these conditions the occurrence of both the oxidation of the V target as well as the saturation of sputtering voltage are guaranteed.

Table 1 Sputtering conditions of VO_x coatings

	Power/ W	Substrate/ target distance	Oxygen flow/ sccm	Temperature/°C
Ti/VO_x	100	75	0·6 0·8 1 1·4 1·6 1·8	400

Structure and texture of VOx thin films

The investigation of the structure and mechanical properties of the vanadium oxides was focused on three O_2 concentrations (0·6, 1 and 1·6 sccm) for which the thicknesses obtained were in order of ~1·4 μm. Figure 2 illustrates the corresponding X-ray diffraction (XRD) patterns under a grazing incidence configuration. Their analysis suggests the presence of the oxygen flowrate effect on the crystallinity of the films. According to the ICDD file no. 00-041-1426, the XRD results confirm that all the coatings had an orthorhombic V_2O_5 structure, as it was envisaged from the preliminary experiments carried out (*see* Fig. 1). Therefore, it could be concluded that the presence of 1 sccm of oxygen in the reactor atmosphere could assure the deposition of a

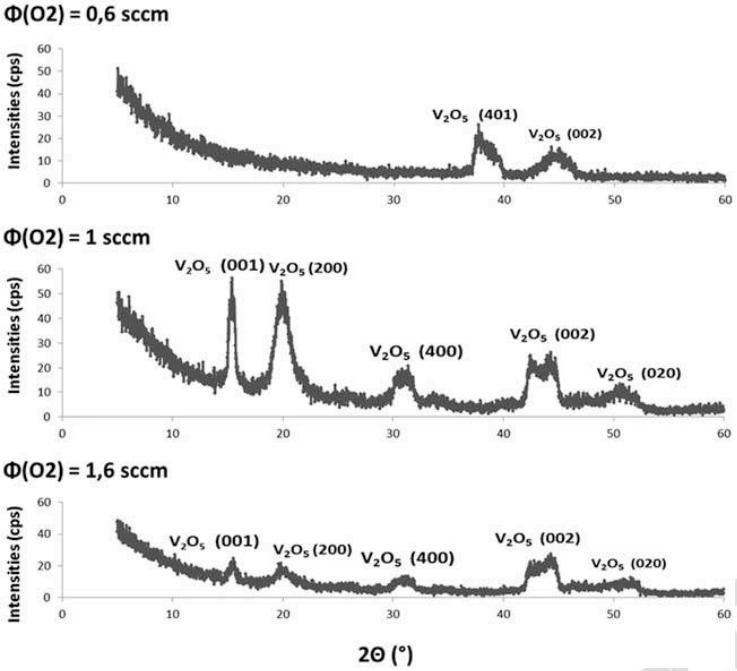

2 XRD patterns under grazing incidence configuration for VO_x thin films deposited at 0·6, 1 and 1·6 sccm O_2

coating with a polycrystalline structure having (001) and (200) orientations. This structure was the most stable phase of the VOx system for the various concentrations of O_2 employed. However, for flowrates less than or greater than 1 sccm, a degeneration of these orientations in the V_2O_5 phase took place. The growth was accompanied by other less intense orientations of the same phase, such as (401) and (020), as well as the presence of other oxygen depleted phases. These results are in agreement with those reported by Huotari *et al.*[22] The use of XRD with a Bragg Brentano geometry allowed the determination of the planes on which a texture study by means of rocking curves had to be performed. The XRD pattern A in Figure 3 shows the diffraction planes (401), (002) and (020) of the V_2O_5 phase for an O_2 concentration of 0·6 sccm. It is worth noting the absence of peaks for the planes (001) and (200). These diffractions are intense and narrow, and therefore, their configurations lead to the analysis of their texture. The rocking curves revealed that only the (401) and (002) diffracted planes were textured (Fig. 3*a*) due to their symmetry around each diffraction angle. When the O_2 concentration was equal to 1 sccm, numerous orientations could be observed, as shown in the XRD pattern represented by B in Fig. 3. This corresponds to a diffraction of the V_2O_5 phase according to the orientations of the planes (200), (001) and (400) at the 2Θ angles: 15·37, 20·017 and 31·014° respectively. Fig. 3*b* illustrates the texture of these planes. According to the orientation of the (200) plane, the V_2O_5 phase appeared to have this pronounced texture, whereas it was much less so for the (001) plane.

When the O_2 concentration in the system was 1·6 sccm, the XRD pattern coincided with the results obtained for an O_2 concentration equal to 0·6 sccm. Indeed, Fig. 3*c* shows the disappearance of peaks exhibiting the plane orientations of (200) and (001) for the V_2O_5 phase. Only the (002) and (020) orientation seemed to maintain a texture, and the rocking curves confirmed a good texture for these planes (Fig. 3*c*)

Table 2 Sputtering voltage behaviour during target presputtering in single Ar gas condition and subsequent co-sputtering in Ar/O2 mixed conditions with O_2 variation flow

Φ O_2/sccm	$P_{O2}/10^{-3}$ mbar	$P_{tot}/10^{-3}$ mbar	Percentage/%	Tension/V
0	0	7·6	0	319
0·4	0	7·6	0	321
0·5	0·02	7·62	0·262467192	323
0·6	0·05	7·65	0·653594771	328
0·7	0·07	7·67	0·912646675	334
0·8	0·07	7·68	0·911458333	341
0·9	0·09	7·69	1·170351105	355
1	0·21	7·81	2·688860435	449
1·01	0·23	7·83	2·937420179	450
1·2	0·55	8·15	6·748466258	471
1·4	0·7	8·3	8·43378494	480
1·6	0·9	8·5	10·58823529	485
1·8	1·1	8·7	12·64367816	488
2	1·25	8·85	14·12429379	489
2·4	1·55	9·15	16·93989071	493
2·8	1·85	9·45	19·57671958	494

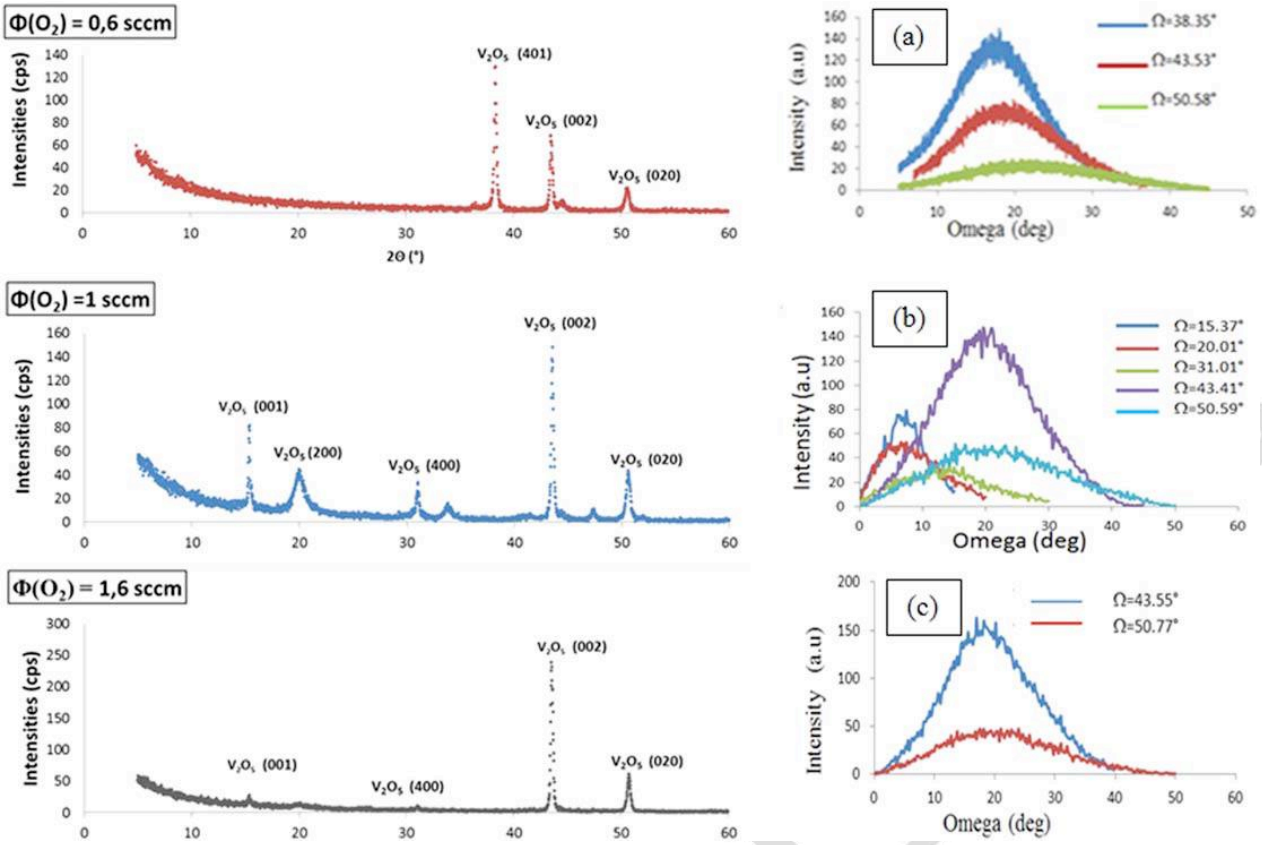

a Bragg Brentano and rocking curves at 0·6 sccm O_2; *b* Bragg Brentano and rocking curves at 1 sccm O_2; *c* Bragg Brentano and rocking curves at 1·6 sccm O_2

3 XRD patterns of VO_x thin films deposited

because of the presence of narrow and symmetric peaks around their representative diffraction angles under the Bragg Brentano configuration. Nevertheless, the crystalline structure is the key factor in determining the electrical, optical, mechanical and tribological properties.

Mechanical properties

The mechanical characterization was conducted by means of nanoindentation, which provided a reliable means of measuring the mechanical properties at a submicron scale. When recording the load as a function of the indentation depth, a hysteresis could be observed between the loading and unloading, which is due to the elastic/plastic deformation during loading. However, during unloading, the plastic deformation remained. The elastic properties were determined from the unloading curve. Although these films showed the same trend during the loading phase, differences were evident during unloading, thus revealing changes in the hardness of the films.

These measurements enabled the determination of the changes in hardness and Young modulus as a function of indenter penetration depth, as well as the corresponding values for the film. Based on the Oliver–Pharr method,[16] the hardness and Young modulus of each deposited coating were determined, and Fig. 4 shows the results as a function of the O_2 concentration. As can be seen, the mechanical properties depend significantly on the O_2 content of the reactant gas present in the deposition chamber. The hardness and Young modulus values varied between 6 and 16·5 GPa and 55 to 152 GPa respectively, as shown in Fig. 5. Although the oxygen supply increased both hardness and Young modulus values, a drop in these parameters was observed when the O_2 concentration exceeded 1 sccm. This trend has also been reported by Lugscheider *et al.*,[23] who studied the influence of O_2 on the mechanical properties of these coatings over a wider range of oxygen concentration. These authors used the magnetron sputtering ion plating process and showed that a maximum hardness of 21 GPa was recorded between 1 and 4 sccm of oxygen. In that case, the decrease was also attributed to the generation of a V_2O_5 phase compound having textures out of the (001) plane or exhibiting phases with depleted oxygen.

Adhesion

Adhesion measurements on thin films of vanadium oxides were carried out by means of scratch testing. The characteristic values of the critical force, determined for the different coated systems as a function of the O_2 concentration level, are shown in Fig. 6. The reported values of Lc_1, Lc_2 Lc_3 correspond to an average of three measurements. As it is well known, the critical force Lc_1 has always been related to the cohesive nature of the coating, corresponding either to the presence of a crack at the edge of the scratch or to the appearance of cracks perpendicular to the scratching direction. The critical force Lc_2 has a rather adhesive nature, leading to coating delamination. The last critical force Lc_3 corresponds to the complete failure of the coating, thus exposing the substrate surface. These critical forces, as it was reported, are also a good indicator of the load bearing capacity, fracture toughness and abrasion resistance of the thin films.[24,25]

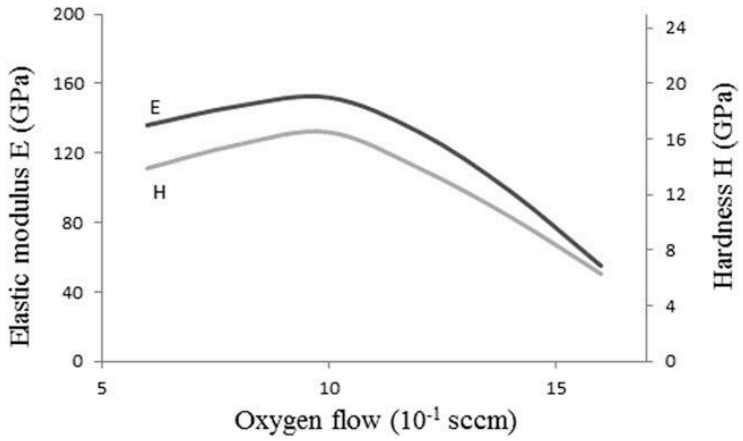

a 0·6, 0·8 and 1 sccm O_2; *b* 1·2, 1·4 and 1·6 sccm O_2

4 Coefficient of friction *vs.* sliding distance and AFM images for VO_x films of varying O_2 concentrations in O_2/Ar gas

It could be observed that all the values corresponding to the critical forces increased slightly up to a concentration of 1 sccm of O_2, clearly demonstrating that coating adhesion is strongly dependent on the oxygen content during its processing. Above this concentration, these values decreased markedly. These results are consistent with those reported by Lugscheider *et al.*,[23] who showed that the adhesion characteristics of VO coatings decrease beyond 1 sccm O_2.

In addition, it is important to mention that a high oxygen amount in the coatings could hinder its diffusivity and also the diffusivity of the metal ions through the already grown oxide layer. Moreover, adhesion forces are dependent on the conductive state of vanadium oxides, as reported by Marwitz *et al.*,[26] who indicated that high conductive layers exhibit low adhesion forces, whereas low conductive layers show higher values of such a parameter.

Wear results

Figure 4 shows the evolution of the coating friction coefficients obtained for various O_2 concentrations, where two different behaviours, depending on the O_2 concentration, can be observed. The first one corresponds to the response to the sliding wear of the coated systems produced with O_2 concentrations up to 1 sccm (Fig. 4*a*), whereas the second response type corresponds to O_2 levels >1 sccm (Fig. 4*b*).

For low oxygen levels (O_2<1 sccm), the coating worn surface, as observed by AFM, appeared more uniform, in comparison with those corresponding to the high O_2 levels (O_2>1 sccm). In this case, the friction coefficient tends to stabilize at a shorter distance (or less number of cycles) than that achieved for the higher oxygen levels coatings. There is a relationship between wear behaviour and dissipated energy needed to achieve a steady state during sliding. As it was pointed out in the literature,[27] the dissipated energy during a sliding contact is caused by a combination of phenomena, which involve an increase in temperature, debonding of worn particles and a change of entropy in relation to the transformation of the two or three bodies in contact. Moreover, Fouvry *et al.*[28] considered that debonding of worn particles is the source of the largest energy dissipation. It follows that the dissipated wear energy to achieve a stabilized friction for the system with an O_2 concentration up to 1 sccm was lower.

Accordingly, any additional information on the worn volume can provide support to the experimental results in relation to the effect of O_2 flow during processing, since the worn volume represented the largest source of energy dissipation. The Archard relation expresses a proportional relationship between the worn volume V and the specific wear coefficient K of the form:

$$V = KFD$$

where F is the normal force, and D is the total sliding distance.

Figure 7 shows the specific wear coefficients as a function of O_2 concentration. It can be seen that the best wear resistance is obtained for the coatings produced when the O_2 concentration is 1 sccm. Above this concentration, the specific wear coefficient increases significantly, which corresponds to the decrease in the hardness values of these coatings.

On the other hand, the difference between the wear performance of the various coatings can be explained by

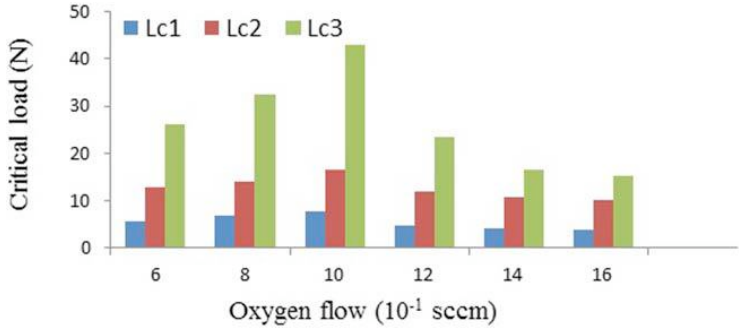

5 Dependence of coating hardness and elastic modulus on O_2 content

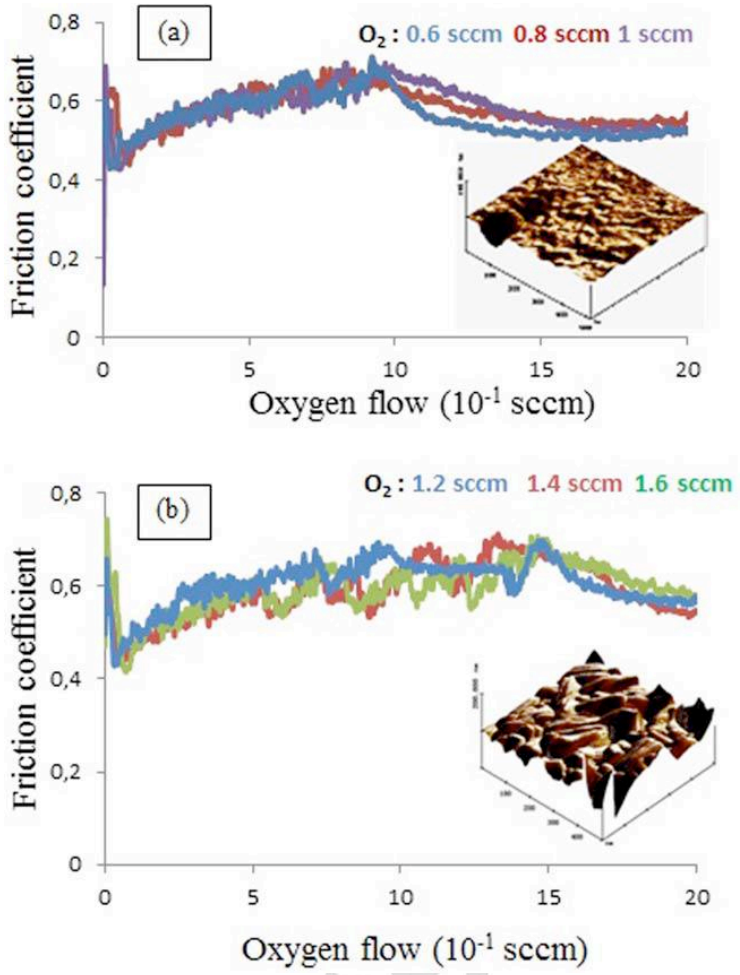

6 Variation of critical loads for VO_x films with varying O_2 concentrations in O_2/Ar gas

taking into account the resistance to plastic deformation described by the relation H^3/E^{*2} (where H represents the hardness, and E^* is the reduced modulus, equal to $E/1-\nu^2$, where ν is Poisson's ratio). The results show that when the O_2 concentration is 1 sccm, such a ratio achieves a value of 0·19, as compared to 0·14 for an O_2 concentration less than or higher than 1 sccm.

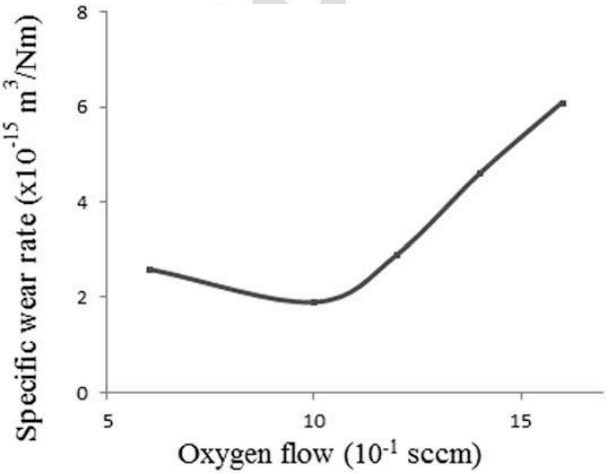

7 Variation of specific wear rate of VO_x films with different O_2 concentrations in O_2/Ar gas mixture

It has to be remembered that the highest wear resistance corresponds to the V_2O_5 phase, which essentially grows along the (200) and (001) planes. Moreover, these coatings did not show any thermal or phase transition during sliding, even at high temperature (600°C) or long sliding times[3]. All these results support the idea that the presence of VO_x provides a good tribological behaviour when low levels of O_2 are present during processing.

By correlating the results of the structural analysis with the mechanical, tribological and adhesion characteristics, it was possible to state that the optimal values for hardness and Young modulus, on the one hand, and those of the wear coefficients and critical adhesion forces, on the other hand, are all related to the nature of the V_2O_5 phase with a strong texture of the (001) planes. The low values of these properties can be attributed to the generation of a phase with textures out of the (001) plane or with oxygen depletion, allowing them to produce voids and other defects within the coating, which could lead to coating softening.

Conclusions

Investigations of VO_x thin films obtained by reactive magnetron sputtering in continuous current mode revealed the direct impact of the O_2 concentration in the sputtering atmosphere, on the coatings structure, texture and mechanical properties. Low partial pressures of O_2 generated a crystalline structure. Any variation of

the O_2 concentration influenced the coating growth rate and growth mechanism. The stoichiometric V_2O_5 can be obtained at 0·6 sccm oxygen flow and by heating the substrate at 400°C in order to accelerate both nucleation and growth mechanisms.

In the O_2 concentration range of the study, the thin film XRD patterns particularly showed the generation of a V_2O_5 Magnéli phase exhibiting different textures. The VO_x layer obtained for a concentration of 1 sccm of O_2 had a pronounced texturing effect for the (001) plane of the V_2O_5 phase, which allowed the best hardness and Young modulus values for this coating.

The oxygen concentration was of great importance with regard to the characterization of the coatings friction, wear and adhesion resistance. The values of specific wear resistance and those of the various critical adhesion forces could be optimized for low levels of O_2, with maximum values at an oxygen flowrate of 1 sccm in the deposition chamber. Finally, it will be interesting to study their tribological behaviour and wear mechanism under elevated temperatures to conclude the lubricious properties.

Acknowledgement

The authors wish to thank Pr. R. Sanjinès (LPMC, EPF Lausanne) for providing the coatings.

References

1. K. Hermann, M. Witko and D. P. Woodruff (eds.): 'The chemical physics of solid surfaces', *Oxide Surf.*, 2001, **9**,136.
2. C. Batista, V. Teixeira and R. M. Ribeiro: 'Materials technology, advanced performance materials', 2011, **26**,1, 35–39.
3. E. Lugscheider, O. Knotek and K. Bobzin: *Surf. Coat. Technol.*, 2000, **133**–**134**, 362–368
4. L. J. Meng, R. A. Silva, H. N. Cui and V. Teixeira: *Thin Solid Films*, 2006, **515**,195.
5. C. Venkatasubramanian, O. M. Cabarcos, W. R. Drawl, D. L. Allara, S. Ashok, M. W. Horn and S. S. N. Bharadwaja: *J. Vac. Sci. Technol. A*, 2011, **29**, 061504.
6. S. P. Lim, J. D. Long, S. Xu and K. Ostrikov: *J. Phys. D*, 2007, **40D**, 1085.
7. S. Beke, L. Korosi, S. Papp, L. Nanai, A. Oszko and J. G. Kiss: *Appl. Surf. Sci.*, 2007, **254**, 1363.
8. A. Kumar, P. Singh, N. Kulkkarni and D. Kaur: *Thin Solid Films*, 2008, **516**, 912.
9. Đ. Goršćak, P. Panjan, M. Čekada and L. Ćurković: *Surf. Coat. Technol.*, 2007, **23**, 177–182.
10. C. Piccirillo, R. Binions and L. P. Parkin: *Thin Solid Films*, 2008, **516**, 1992.
11. S. Beke: *Thin Solid Films*, 2011, **519**, 1761–1771.
12. Y. S. Yoon, J. S. Kim and S. H. Choi: *Thin Solid Films*, 2004, **460**, 41–47.
13. J. W. Lee, S. R. Min and H. N. Cho: *Thin Solid Films*, 2007, **515**, 7740–7743.
14. R. B. Laxane, R. S. Bhide, A. S. Patil and S. G. Sane: *Surf. Eng.*, 2006, 78–80.
15. E. Lugscheider, O. Knotek, S. Barwulf and K. Bobzin: *Surf. Coat. Technol.*, 2001, **142**–**144**, 137–142.
16. W. C. Oliver and G. M. Pharr: *J. Mater. Res.*, 1992, **7**, 1564–1582.
17. B. D. Beake, V. M. Valizadeh and J. S. Colligon: *J. Phys. D*, 2006, **39D**, 1392.
18. A. R. Bushroa, H. H. Masjuki, M. R. Muhamad and B. D. Beake: *Surf. Coat. Technol.*, 2011, **206**, 1837–1844.
19. J. Li and W. Beres: *Can. Metall. Q.*, 2007, **46**, 155–173.
20. D.-A. Mendels: *Tribol. Mater. Surf. Interfaces*, 2008, **2**, 232–244.
21. X. Wei, S. Li, J. Gou, X. Dong, X. Yang, W. Li, T. Wang, Z. Wu, Y. Jiang and Z. Chen: *Opt. Mater.*, 2014, **36**, 1419–1423
22. J. Huotari, J. Lappalainen, J. Puustinen and A. Lloyd Spetz: *Sens. Actuators B*, 2013, **187B**, 386–394.
23. E. Lugscheider, S. Barwulf and C. Barimani: *Surf. Coat. Technol.*, 1999, **120–121**, 458–464.
24. J. Xu, Z.-H. Xie and P. Munroe: *Intermetallics*, 2011, **19**, 1146–1156.
25. X. Ma and A. Matthews: *Surf. Coat. Technol.*, 2007, **202**, 1214–1220.
26. C. Marwitz, B. Stegemann, M. Breitkreitz, D. Spaltmann, H. Kloss, M. Woydt and H. Sturm: *Surf. Sci.*, 2011, **605**, 1271–1274
27. A. Ramalho and J. C. Miranda: *Wear*, 2006, **260**, 361–367.
28. S. Fouvry, T. Liskiewicz, P. Kapsa, S. Hannel and E. Sauger: *Wear*, 2003, **255**, 287–298.